

Relativistic electron PXR and FPXR yield ratio

S Blazhevich, A Noskov
Belgorod State University, Belgorod, Russia

E-mail: blazh@bsu.edu.ru

Abstract. The parametric X-radiation of relativistic electron crossing a single crystal plate is considered on the basis of dynamic diffraction theory in Laue geometry both in Bragg (PXR) and forward (FPXR) directions. Analytical expressions for spectral-angular density of these radiations in indicated directions are derived in general case of electron coulomb field asymmetric reflection from the target surface. The ratio of contributions of these radiation mechanisms into the total yield of the radiation is investigated. It is shown that the ratio of contributions of these radiation mechanisms can change sharply depending on the value of the reflection asymmetry.

1. Introduction

When a fast charged particle crosses a single crystal, its coulomb field scatters on the system of parallel atomic planes generating parametric X-radiation (PXR) [1-3]. The theory of PXR of relativistic particle in a crystal forecasts the radiation not only in Bragg scattering direction, but also in the direction of radiating particle velocity (FPXR) [4-6], which represents an appearance of dynamical diffraction in PXR. It is known that some attempts of the FPXR experimental research were made [7-11], but the first report about its experimental discovery has appeared recently in ref. [10], where the method of TR background suppression was used in vicinity of Bragg frequency based on destructive interference of TR generated on the entrance and on the escape surfaces of the crystal plate (as target) accordingly. But a spectrally narrow peak arisen near Bragg frequency due to dynamical diffraction [12], which could take place in the FPXR experiment was not analyzed in the work [10]. In the experiment [11] the relativistic electron X-radiation was registered from a thick single non-absorptive crystal target in the condition of FPXR generation, nevertheless the sought-for peak became weakly apparent on the background of the radiation generated by scattered electrons in the structural material of the experimental setup. Thus the theoretical investigations of FPXR properties and the optimization of viewing conditions for experimental observation of this dynamical effect remain topical up to date.

The detailed theoretical description of dynamical effect of FPXR and its accompanying transition radiation (TR), as a background, was done for the case of symmetrical reflection in the works [13-15]. Under condition of asymmetrical reflection of the relativistic electron coulomb field the PXR and TR were theoretically investigated in ref.-s [16-18] and FPXR in Bragg geometry in ref. [19]. The above-mentioned works showed that the spectral-angular density of these radiation mechanisms depends essentially on the reflection asymmetry and revealed the effects associated with it.

In the present work the analytical expressions for spectral-angular density of FPXR is derived in the framework of two-wave approximation of dynamic diffraction theory [20] in general case of asymmetrical field reflection. An expression for spectra-angular density of PXR was derived recently

in the work [17] describing the dependence of the radiation parameters on reflection asymmetry. In the present work on the basis of the expressions obtained the ratio of FPXR and PXR yield was investigated depending on the angle between the reflecting atomic planes and crystal plate surface, i.e. on the reflection asymmetry.

2. FPXR amplitude

Let us consider the radiation of a fast charged particle crossing a single crystal plate with a constant velocity \mathbf{V} (look in figure 1.) We will use the same table of symbols as in the work [17].

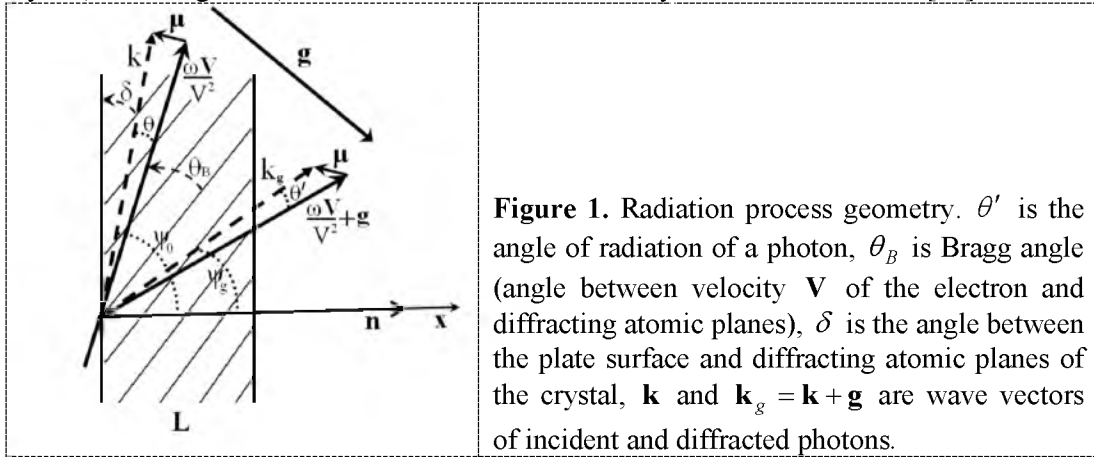


Figure 1. Radiation process geometry. θ' is the angle of radiation of a photon, θ_B is Bragg angle (angle between velocity \mathbf{V} of the electron and diffracting atomic planes), δ is the angle between the plate surface and diffracting atomic planes of the crystal, \mathbf{k} and $\mathbf{k}_g = \mathbf{k} + \mathbf{g}$ are wave vectors of incident and diffracted photons.

While solving the problem, let us consider an equation for a Fourier image of an electromagnetic field

$$\mathbf{E}(\mathbf{k}, \omega) = \int dt d^3 r \mathbf{E}(\mathbf{r}, t) \exp(i\omega t - i\mathbf{k}\mathbf{r}) \quad (1)$$

Since the field of a relativistic particle could, to a good accuracy, be taken as being transverse, the incident $\mathbf{E}_0(\mathbf{k}, \omega)$ and diffracted $\mathbf{E}_g(\mathbf{k}, \omega)$ electromagnetic waves are determined by two amplitudes with different values of transverse polarization

$$\begin{aligned} \mathbf{E}_0(\mathbf{k}, \omega) &= E_0^{(1)}(\mathbf{k}, \omega) \mathbf{e}_0^{(1)} + E_0^{(2)}(\mathbf{k}, \omega) \mathbf{e}_0^{(2)}, \\ \mathbf{E}_g(\mathbf{k}, \omega) &= E_g^{(1)}(\mathbf{k}, \omega) \mathbf{e}_1^{(1)} + E_g^{(2)}(\mathbf{k}, \omega) \mathbf{e}_1^{(2)}. \end{aligned} \quad (2)$$

The unit vectors of polarization $\mathbf{e}_0^{(1)}$, $\mathbf{e}_0^{(2)}$, $\mathbf{e}_1^{(1)}$ and $\mathbf{e}_1^{(2)}$ are chosen in the following way. Vectors $\mathbf{e}_0^{(1)}$ and $\mathbf{e}_0^{(2)}$ are perpendicular to vector \mathbf{k} , and vectors $\mathbf{e}_1^{(1)}$ and $\mathbf{e}_1^{(2)}$ are perpendicular to vector $\mathbf{k}_g = \mathbf{k} + \mathbf{g}$. Vectors $\mathbf{e}_0^{(2)}$, $\mathbf{e}_1^{(2)}$ are situated on the plane of vectors \mathbf{k} и \mathbf{k}_g (π -polarization) and $\mathbf{e}_0^{(1)}$, $\mathbf{e}_1^{(1)}$ are perpendicular to this plane (σ -polarization); \mathbf{g} is vector of the reciprocal lattice, defining a set of reflecting atomic planes. The system of equation for the Fourier transform images of electromagnetic field in two-wave approximation of dynamic theory of diffraction has the following view [21]:

$$\begin{cases} (\omega^2(1 + \chi_0) - k^2)E_0^{(s)} + \omega^2 \chi_{-\mathbf{g}} C^{(s,\tau)} E_g^{(s)} = 8\pi^2 i e \omega \theta V P^{(s)} \delta(\omega - \mathbf{k}\mathbf{V}), \\ \omega^2 \chi_{\mathbf{g}} C^{(s,\tau)} E_0^{(s)} + (\omega^2(1 + \chi_0) - k_g^2)E_g^{(s)} = 0, \end{cases} \quad (3)$$

where $\chi_0 = \chi_0' + i\chi_0''$ is the average dielectric susceptibility, $\chi_{\mathbf{g}}$, $\chi_{-\mathbf{g}}$ are the coefficients of the Fourier expansion of the dielectric susceptibility of a crystal over the reciprocal lattice vectors \mathbf{g} .

The values $C^{(s)}$ and $P^{(s)}$ are defined in the system (3) as

$$C^{(s)} = \mathbf{e}_0^{(s)} \mathbf{e}_1^{(s)}, \quad C^{(1)} = 1, \quad C^{(2)} = \cos 2\theta_B, \quad P^{(s)} = \mathbf{e}_0^{(s)} (\boldsymbol{\mu} / \mu), \quad P^{(1)} = \sin \varphi, \quad P^{(2)} = \cos \varphi. \quad (4)$$

$\boldsymbol{\mu} = \mathbf{k} - \omega \mathbf{V}/V^2$ is the virtual photon momentum vector component perpendicular to particle velocity vector V ($\mu = \omega\theta/V$, where $\theta \ll 1$ is the angle between vectors k and V), θ_B is the angle between electron velocity and a set of atomic planes in the crystal (Bragg angle), φ is the azimuth angle, counted off from the plane formed by vectors V and \mathbf{g} , the value of the reciprocal lattice vector is shown by expression $g = 2\omega_B \sin\theta_B/V$, ω_B is Bragg's frequency. The angle between vector $\frac{\omega \mathbf{V}}{V^2} + \mathbf{g}$ and diffracted wave vector k_g is defined as θ' . The equation system (3) under $s = 1$ describes the fields of σ -polarization, and under $s = 2$ the fields of π -polarization.

Let us solve the dispersion equation for x-waves in crystal following from the system (3) :

$$(\omega^2(1+\chi_0) - k^2)(\omega^2(1+\chi_0) - k_g^2) - \omega^4 \chi_{-g} \chi_g C^{(s)2} = 0, \quad (5)$$

using standard methods of dynamic theory [20].

Let us search for the wave vectors projection k and k_g to the axis X, aligned with the vector n (see figure 1.) as:

$$k_x = \omega \cos\psi_0 + \frac{\omega\chi_0}{2\cos\psi_0} + \frac{\lambda_0}{\cos\psi_0}, \quad k_{gx} = \omega \cos\psi_g + \frac{\omega\chi_0}{2\cos\psi_g} + \frac{\lambda_g}{\cos\psi_g}. \quad (6)$$

For this purpose we will use the well-known relation, connecting dynamic addition agents λ_0 and λ_g for X-waves [20]:

$$\lambda_g = \frac{\omega\beta}{2} + \lambda_0 \frac{\gamma_g}{\gamma_0}, \quad (7)$$

where $\beta = \alpha - \chi_0 \left(1 - \frac{\gamma_g}{\gamma_0}\right)$, $\alpha = \frac{1}{\omega^2}(k_g^2 - k^2)$, $\gamma_0 = \cos\psi_0$, $\gamma_g = \cos\psi_g$, ψ_0 is the angle between incident wave vector k and vector normal to the plate surface n , ψ_g is the angle between wave vector k_g and the vector n (see figure 1). The modules of vectors k and k_g are:

$$k = \omega\sqrt{1+\chi_0} + \lambda_0, \quad k_g = \omega\sqrt{1+\chi_0} + \lambda_g. \quad (8)$$

Assumed that $k_{||} \approx \omega \sin\psi_0$ and $k_{g||} \approx \omega \sin\psi_g$, we will obtain

$$\lambda_0^{(1,2)} = \omega \frac{\gamma_0}{4\gamma_g} \left(-\beta \pm \sqrt{\beta^2 + 4\chi_g \chi_{-g} C^{(s)2} \frac{\gamma_g}{\gamma_0}} \right), \quad (9)$$

$$\lambda_g^{(1,2)} = \frac{\omega}{4} \left(\beta \pm \sqrt{\beta^2 + 4\chi_g \chi_{-g} C^{(s)2} \frac{\gamma_g}{\gamma_0}} \right). \quad (10)$$

As $|\lambda_0| \ll \omega$ and $|\lambda_g| \ll \omega$, we can show that $\theta \approx \theta'$ (see in figure 1), and hereinafter will use θ in the all occasions.

The solution of the combined equations (3) gives us the relativistic particle field in the vacuum in front of the crystal as

$$E_0^{(s)vacI} = \frac{8\pi^2 ieV\theta P^{(s)}}{\omega} \frac{1}{(\gamma_0 / \gamma_g)(-\chi_0 - 2\lambda_g \gamma_0 / \omega \gamma_g + \beta \gamma_0 / \gamma_g)} \delta(\lambda_g - \lambda_g^*), \quad (11)$$

the same field inside the crystal as

$$E_0^{(s)cr} = \frac{8\pi^2 ieV\theta P^{(s)}}{\omega} \frac{-\omega^2 \beta - 2\omega \lambda_0 \gamma_g / \gamma_0}{4(\gamma_g / \gamma_0)(\lambda_0 - \lambda_0^{(1)})(\lambda_0 - \lambda_0^{(2)})} \delta(\lambda_0 - \lambda_0^*) + E_0^{(s)1} \delta(\lambda_0 - \lambda_0^{(1)}) + E_0^{(s)2} \delta(\lambda_0 - \lambda_0^{(2)}) \quad (12)$$

and the field in the vacuum behind the crystal as

$$E_0^{(s)vacII} = \frac{8\pi^2 ieV\theta P^{(s)}}{\omega} \frac{1}{-\chi_0 - 2\lambda_0 / \omega} \delta(\lambda_0 - \lambda_0^*) + E_0^{(s)Rad} \delta(\lambda_0 + \omega \chi_0 / 2), \quad (13)$$

where $E_0^{(s)Rad}$ is the coherent radiation amplitude in the electron velocity direction.

The following expression bounding the diffracted and incident fields inside of the crystal results from second equation of system (3):

$$E_0^{(s)cr} = (2\omega \lambda_g / \omega^2 \chi_g C^{(s)}) E_g^{(s)cr}. \quad (14)$$

For definition of amplitude $E_0^{(s)Rad}$ we will use the ordinary boundary conditions on the inlet and outlet surfaces of the crystal plate:

$$\int E_0^{(s)vacI} d\lambda_0 = \int E_0^{(s)cr} d\lambda_0, \quad \int E_g^{(s)cr} d\lambda_0 = 0, \quad \int E_0^{(s)cr} \exp(i(\lambda_0 / \gamma_0)L) d\lambda_0 = \int E_0^{(s)vacII} \exp(i(\lambda_0 / \gamma_0)L) d\lambda_0. \quad (15)$$

Hence we will obtain the expression for the field of the radiation:

$$E_0^{(s)Rad} = \frac{8\pi^2 ieV\theta P^{(s)}}{\omega} \frac{\exp\left[i(\omega \chi_0 / 2 + \lambda_g^*)L / \gamma_g\right]}{2(\gamma_g / \gamma_0)(\lambda_0^{(1)} - \lambda_0^{(2)})} \times \left[\left(-\omega^2 \beta - 2\omega \lambda_0^{(2)} \gamma_g / \gamma_0\right) \left(-\omega \chi_0 - 2\lambda_0^*\right)^{-1} + \left(2(\lambda_0^* - \lambda_0^{(2)})\right)^{-1} \right] \left(\exp(iL(\lambda_0^{(2)} - \lambda_0^*) / \gamma_0) - 1\right) - \left(-\omega^2 \beta - 2\omega \lambda_0^{(1)} \gamma_g / \gamma_0\right) \left(-\omega \chi_0 - 2\lambda_0^*\right)^{-1} + \left(2(\lambda_0^* - \lambda_0^{(1)})\right)^{-1} \right] \left(\exp(iL(\lambda_0^{(1)} - \lambda_0^*) / \gamma_0) - 1\right). \quad (16)$$

The terms in square brackets in (16) correspond to two branches of solution for X-ray waves excited in the crystal.

To make the FPXR reflex appear, at least one of the following inequalities must be hold:

$$\operatorname{Re}(\lambda_0^* - \lambda_0^{(1)}) = 0, \quad \operatorname{Re}(\lambda_0^* - \lambda_0^{(2)}) = 0, \quad (17)$$

i.e., in (16) the real part of denominator of at least one of the terms in square bracket must be vanishing. For the further analyses we will represent the dynamic addition (9) in the following view:

$$\lambda_0^{(1,2)} = (\omega \chi_g' | C^{(s)} / 2\varepsilon) \left(-\xi^{(s)} + i\rho^{(s)}(1 - \varepsilon) / 2 \pm \sqrt{\xi^{(s)2} + \varepsilon - 2i\rho^{(s)} \left((1 - \varepsilon)\xi^{(s)} / 2 + \kappa^{(s)}\varepsilon \right) - \rho^{(s)2} \left((1 - \varepsilon)^2 / 4 + \kappa^{(s)2} \varepsilon \right)} \right), \quad (18)$$

where

$$\rho^{(s)} = \chi_0'' / |\chi_g'| C^{(s)}, \quad \varepsilon = \cos \psi_g / \cos \psi_0, \quad \kappa^{(s)} = \chi_g'' C^{(s)} / \chi_0'', \quad \xi^{(s)} = \eta^{(s)}(\omega) + (1 + \varepsilon) / 2\nu^{(s)},$$

$$\eta^{(s)}(\omega) = (2 \sin^2 \theta_B / |\chi_g'| C^{(s)}) (\omega_B (1 + \theta \cos \varphi \cot \theta_B) / \omega - 1).$$

The asymmetry parameter ε can be represented as $\varepsilon = \sin(\delta + \theta_B) / \sin(\delta - \theta_B)$, where θ_B is the angle between electron velocity and diffracting atomic plane. Hence we can see that parameter ε increases when the angle of electron incidence $\delta - \theta_B$ decreases and vice versa (see figure 2).

Since in the region of X-ray frequencies the inequality $2 \sin^2 \theta_B / V^2 |\chi_g'| C^{(s)} \gg 1$ is satisfied, then $\eta^{(s)}(\omega)$ is a fast function of the frequency ω , so for further analysis of the properties of the PXR spectra it is convenient to treat $\eta^{(s)}(\omega)$ as a spectral variable characterizing the frequency ω .

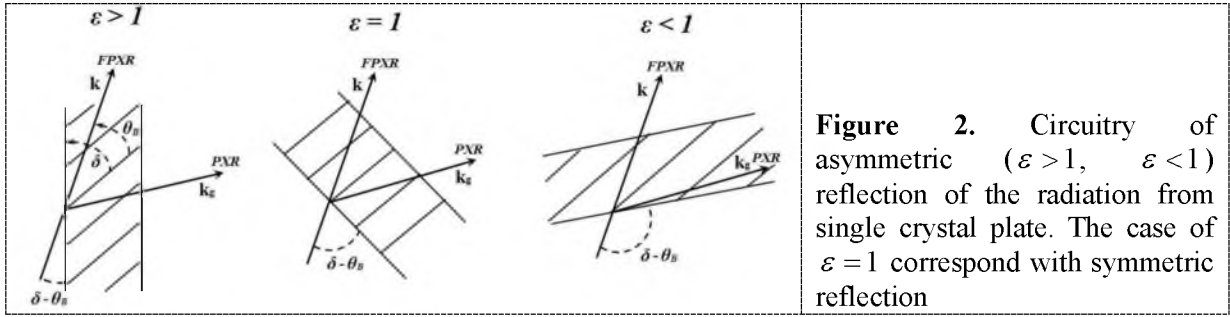


Figure 2. Circuitry of asymmetric ($\varepsilon > 1$, $\varepsilon < 1$) reflection of the radiation from single crystal plate. The case of $\varepsilon = 1$ correspond with symmetric reflection

Using (18) let us represent the expression for field amplitude of radiation along the electron velocity vector as two summands:

$$E_0^{(s)Rad} = E_{FPXR}^{(s)} + E_{TR}^{(s)}, \quad (19a)$$

$$E_{FPXR}^{(s)} = \frac{4\pi^2 ieV}{\omega} \frac{\theta P^{(s)}}{\gamma^{-2} + \theta^2 - \chi_0} \frac{1}{\sqrt{\xi^{(s)^2} + \varepsilon}} \times$$

$$\times \left(\frac{1 - \exp[-ib^{(s)}\Sigma^{(2)} - b^{(s)}\rho^{(s)}\Delta^{(2)}]}{\Sigma^{(2)} - i\rho^{(s)}\Delta^{(2)}} - \frac{1 - \exp[-ib^{(s)}\Sigma^{(1)} - b^{(s)}\rho^{(s)}\Delta^{(1)}]}{\Sigma^{(1)} - i\rho^{(s)}\Delta^{(1)}} \right) \exp[i\omega L(\gamma^{-2} + \theta^2) / 2\gamma_0]$$

(19b)

$$E_{TR}^{(s)} = \frac{4\pi^2 ieV\theta P^{(s)}}{\omega} \left(\frac{1}{\gamma^{-2} + \theta^2} - \frac{1}{\gamma^{-2} + \theta^2 - \chi_0} \right) \times$$

$$\left(\left(1 - \xi^{(s)} / \sqrt{\xi^{(s)^2} + \varepsilon} \right) \left(1 - \exp[-ib^{(s)}\Sigma^{(2)} - b^{(s)}\rho^{(s)}\Delta^{(2)}] \right) + \right.$$

$$\left. + \left(1 + \xi^{(s)} / \sqrt{\xi^{(s)^2} + \varepsilon} \right) \left(1 - \exp[-ib^{(s)}\Sigma^{(1)} - b^{(s)}\rho^{(s)}\Delta^{(1)}] \right) \right) \exp[i\omega L(\gamma^{-2} + \theta^2) / 2\gamma_0]$$

(19c)

where

$$\Delta^{(1,2)} = (\varepsilon + 1) / 2\varepsilon \mp (1 - \varepsilon)\xi^{(s)} / 2\varepsilon\sqrt{\xi^{(s)^2} + \varepsilon} \mp \kappa^{(s)} / \sqrt{\xi^{(s)^2} + \varepsilon},$$

$$\Sigma^{(1)} = \sigma^{(s)} + \left(\xi^{(s)} - \sqrt{\xi^{(s)^2} + \varepsilon} \right) / \varepsilon, \quad \Sigma^{(2)} = \sigma^{(s)} + \left(\xi^{(s)} + \sqrt{\xi^{(s)^2} + \varepsilon} \right) / \varepsilon.$$

$$\sigma^{(s)} = (\theta^2 + \gamma^{-2} - \chi_0') / |\chi_g'| C^{(s)} \equiv (\theta^2 / |\chi_0'| + \gamma^{-2} / |\chi_0'| + 1) / \nu^{(s)}, \quad \nu^{(s)} = |\chi_g'| C^{(s)} / |\chi_0'|$$

$$b^{(s)} = \omega |\chi_g'| C^{(s)} L / 2\gamma_0.$$

(20)

Parameter $b^{(s)}$ can be presented in view

$$b^{(s)} = L / 2 \sin(\delta - \theta_B) L_{ext}^{(s)} .$$

Hence it follows that parameter $b^{(s)}$ is equal to half of the relativistic electron path length in the plate expressed in extinction lengths.

The expression (19b) represents the field amplitude for FPXR, and (19c) represents the TR generated on inlet and outlet surfaces of the plate. The FPXR yield is formed basically at the expense of one of the branches in the solution for X-ray waves generated in the crystal that corresponds to the second summand in (19b) because only there the real part of the denominator must be vanishing:

$$\Sigma^{(1)} \equiv \sigma^{(s)} + \left(\xi^{(s)} - \sqrt{\xi^{(s)2} + \varepsilon} \right) / \varepsilon = 0 . \quad (21)$$

The equation (21) solution defines a frequency ω_* in whose vicinity the spectrum of FPXR photons radiated at a fixed observation angle is concentrated.

We will consider the case of a thin target ($b^{(s)} \rho^{(s)} \ll 1$) when the absorption coefficient $\rho^{(s)}$ can be neglected. For the graphic extraction of dynamical effects in coherent radiation processes we will use a crystal plate of such a thickness L that the electron path in the plate $L / \sin(\delta - \theta_B)$ will much exceed the extinction length $L_{ext}^{(s)} = 1 / \omega |\chi_g'| C^{(s)}$ of x-ray waves in the crystal, i.e. $b^{(s)} \gg 1$.

3. Spectral-angular density of FPXR

Substituting (19b) into the well known [21] expression for spectral-angular X-radiation density

$$\omega \frac{d^2 N}{d\omega d\Omega} = \omega^2 (2\pi)^{-6} \sum_{s=1}^2 \left| E_0^{(s)Rad} \right|^2 \quad (22)$$

we will obtain for thin crystal the expressions, accordingly describing the contributions of FPXR:

$$\omega \frac{d^2 N_{FPXR}^{(s)}}{d\omega d\Omega} = \frac{e^2}{4\pi^2} P^{(s)2} \frac{\theta^2}{(\theta^2 + \gamma^{-2} - \chi_0')^2} R_{FPXR}^{(s)} , \quad (23a)$$

$$R_{FPXR}^{(s)} = \frac{4}{\xi^{(s)2} + \varepsilon} \sin^2 \left(\frac{b^{(s)}}{2} \left(\sigma^{(s)} + \left(\xi^{(s)} - \sqrt{\xi^{(s)2} + \varepsilon} \right) / \varepsilon \right) \right) \left(\sigma^{(s)} + \left(\xi^{(s)} - \sqrt{\xi^{(s)2} + \varepsilon} \right) / \varepsilon \right)^{-2} , \quad (23b)$$

The expressions obtained (23) are the main result of the present work, as they let us investigate all the spectral-angular characteristics of FPXR.

4. Spectral-angular density of the radiation in Bragg direction

The expression describing the contributions of FPXR was obtained in the work [17]:

$$\omega \frac{d^2 N_{PXR}^{(s)}}{d\omega d\Omega} = \frac{e^2}{4\pi^2} P^{(s)2} \frac{\theta^2}{(\theta^2 + \gamma^{-2} - \chi_0')^2} R_{PXR}^{(s)} , \quad (24a)$$

$$R_{PXR}^{(s)} = 4 \left(1 - \frac{\xi^{(s)}}{\sqrt{\xi^{(s)2} + \varepsilon}} \right)^2 \sin^2 \left(\frac{b^{(s)}}{2} \left(\sigma^{(s)} + \left(\xi^{(s)} - \sqrt{\xi^{(s)2} + \varepsilon} \right) / \varepsilon \right) \right) \left(\sigma^{(s)} + \left(\xi^{(s)} - \sqrt{\xi^{(s)2} + \varepsilon} \right) / \varepsilon \right)^{-2} . \quad (24b)$$

5. Ratio of the PXR and FPXR yields

The PXR and FPXR spectra described accordingly by $R_{PXR}^{(s)}$ and $R_{FPXR}^{(s)}$ depend on parameter ε , therefore the effect of asymmetry on the ratio of these radiation yields derived from (23b) and (24b) is of interest:

$$R_{PXR}^{(s)} / R_{FPXR}^{(s)} = \left(\sqrt{\xi^{(s)^2} + \varepsilon} - \xi^{(s)} \right)^2 \quad (25)$$

When the asymmetry parameter ε decreases, i.e. the angle $\delta - \theta_B$ of the relativistic electron incident on the crystal target surface increases (see in figure 2), the PXR in forward direction (FPXR) intensity increases and can considerably exceed the PXR in Bragg direction.

$$R_{PXR}^{(s)} \ll R_{FPXR}^{(s)} \quad (26)$$

Let us consider how the intensity of each of the radiations changes separately. The curves calculated by formulas (23b) and (24b) and represented in figure 3 show that the FPXR peak amplitude increases and that of PXR decreases when parameter ε decreases. The curves in figure 3 are plotted for fixed values of the observation angle, the length of path and the energy of the radiating particle.

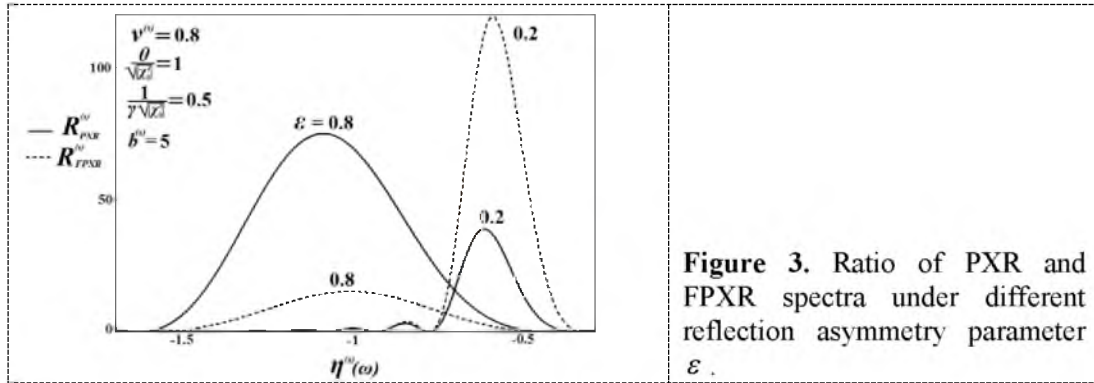


Figure 3. Ratio of PXR and FPXR spectra under different reflection asymmetry parameter ε .

The ratio (25) also depends on observation angle θ , radiating particle energy defined by Lorentz factor γ and parameter $\nu^{(s)}$. Using (21) we will find the expression for frequency ω_* near which spectrum of FPXR is concentrated and write the ratio (25) for that frequency:

$$R_{PXR}^{(s)} / R_{FPXR}^{(s)} = \varepsilon^2 \left(\theta^2 / |\chi'_0| + \gamma^{-2} / |\chi'_0| + 1 \right)^2 / \nu^{(s)^2} \quad (27)$$

In maximum of the parametric radiation angular density, when $\theta = \sqrt{\gamma^{-2} + |\chi'_0|}$ this ratio will have the following view:

$$R_{PXR}^{(s)} / R_{FPXR}^{(s)} = 2\varepsilon^2 \left(\gamma^{-2} / |\chi'_0| + 1 \right)^2 / \nu^{(s)^2} \quad (28)$$

As the value of parameter $\nu^{(s)}$ is always less than unity, it results from (28) that when $\gamma^2 |\chi'_0| \ll 1$ than PXR yield will exceed the yield of FPXR. In the case when $\gamma^2 |\chi'_0| \geq 1$ (or even some less than unity) the ratio (28) will strongly depend on asymmetry parameter ε .

To consider the influence of the reflection asymmetry on the ratio of angular densities of these radiations we will integrate the expression (23) and (24) over frequency function $\eta^{(s)}(\omega)$:

$$\frac{dN_i^{(s)}}{d\Omega} = \frac{e^2 P^{(s)^2}}{8\pi^2 \sin^2 \theta_B} F_i^{(s)}, \quad F_i^{(s)} = \nu^{(s)} \left[\frac{\theta^2}{|\chi'_0|} / \left(\frac{\theta^2}{|\chi'_0|} + \frac{1}{\gamma^2 |\chi'_0|} + 1 \right) \right]^2 \int_{-\infty}^{+\infty} R_i^{(s)} d\eta^{(s)}(\omega) \quad (29)$$

$$i = PXR, FPXR$$

The curves describing the angular density of PXR and FPXR plotted by formulas (29) are presented in figure 4 and figure 5. It is evident from these figures, that under condition $\varepsilon \ll 1$ the angular density of FPXR considerably exceeds the density of PXR.

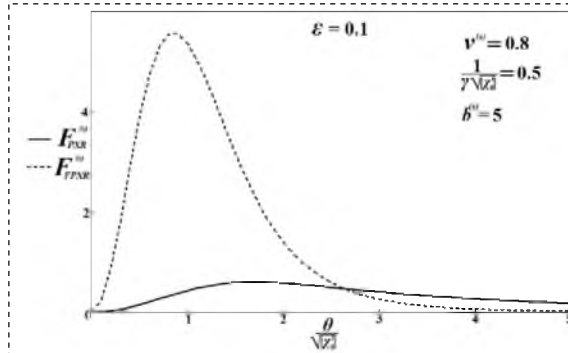


Figure 4. PXR and FPXR angular density under condition of reflection asymmetry (parameter $\varepsilon = 0.1$).

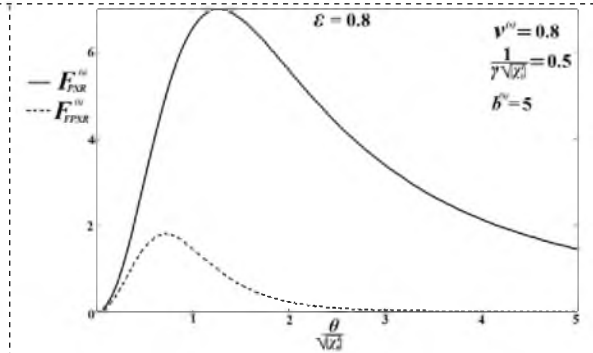


Figure 5. The same as in Fig.4 for another reflection asymmetry ($\varepsilon = 0.8$).

Conclusion

Based on two-wave approximation of the dynamic scattering theory, forward parametric X-ray radiation (FPXR) of a relativistic electron is investigated in a single crystal plate in a Laue scattering geometry. Analytical expressions for the spectral-angular distribution of FPXR and transition radiation (TR) are derived in general case of asymmetric reflection. It is shown that under fixed Bragg angle θ_B and path length $2b^{(s)}$ of relativistic electron in the crystal plate the ratio of FPXR and PXR yields considerably depends on the angle between reflected atomic planes and inlet surface of the plate δ , i.e. on reflection asymmetry parameter $\varepsilon = \sin(\delta + \theta_B) / \sin(\delta - \theta_B)$, at that in the case where the angle of the electron incidence on the surface of the crystal plate $\delta - \theta_B$ increases (i.e. ε decreases) the spectral-angular density of PXR decreases and that of FPXR increases and can exceed the density of PXR. In the present work the ratio of FPXR and PXR yields was investigated and it was shown that this ratio significantly depends on the reflection asymmetry, at that with decreasing asymmetry parameter ε the FPXR relative contribution increases for any observation angle. The results obtained can be used when preparing the experimental investigations of FPXR.

References

- [1] Ter-Mikaelian M 1972 *High-Energy Electromagnetic Process in Condensed Media* (New York : Wiley)
- [2] Garibian G, Yang C 1971 J. Exp. Theor. Phys. **61** 930
- [3] Baryshevsky V, Feranchuk I 1971 J. Exp. Theor. Phys. **61** 944
- [4] Garibian G, Yang C 1972 J. Exp. Theor. Phys. **63** 1198
- [5] Baryshevsky V, Feranchuk I 1976 Phys. Lett. A **57** 183
- [6] Baryshevsky V, Feranchuk I 1983 J. Physique (Paris) **44** 913
- [7] Yuan Luke C, Alley P, Bamberger A et al. 1985 Nucl. Instr. and Meth. In Phys. Res. A **234** 426
- [8] Kalinin B, Naumenko G, Padalko D et al. 2001 Nucl. Instr. and Meth. In Phys. Res. B **173** 253
- [9] Kube G, Ay C, Backe H, Clawiter N at al. 2001 in Abstracts V International Symposium "Radiation from Relativistic Electrons in Periodic Structures", Lake Aya, Altai Mountains, Russia, 10-14 September
- [10] Backe H, Clawiter N 2003 at al, in Proc. Of the Intern. Symp. on Channeling –Bent Crystals – Radiation Processes, , Frankfurt am Main, Germany, EP Systema Bt., Debrecen, p.41.
- [11] Aleinik A, Baldin A, Bogomasova E, Vnukov I at al. 2004 J. Exp. Theor. Phys Letters **80** 447
- [12] Imanishi N, Nasonov N, and Yajima K 2001 Nucl. Instr. And Meth. In Phys. Res. B **173** 227
- [13] Kubankin A, Nasonov N, Sergienko V, Vnukov I 2003 Nucl. Instr. and Meth. In Phys. Res. B **201** 97

- [14] Nasonov N, Noskov A 2003 Nucl. Instr. Meth. In Phys. Res. B **201** 67
- [15] Kubankin A, Nasonov N, Noskov A, 2002 in Proc. 7 Int. Russian-Japanese Symposium “Interaction of fast charged particles with solids”, Nov. 24-30, Kyoto, Japan, p.217-225
- [16] Blazhevich S, Noskov A 2006 Nucl. Instr. Meth. In Phys. Res. B **252** 69
- [17] Blazhevich S, Noskov A 2008 Nucl. Instr. Meth. In Phys. Res. B **266** 3770
- [18] Blazhevich S, Noskov A 2008 Nucl. Instr. Meth. In Phys. Res. B **266** 3777
- [19] Blazhevich S, Noskov A 2006 Russian Physics Journal **50** 574
- [20] Pinsker Z 1984 *Dynamic Scattering of X-rays in Crystals* (Berlin: Springer)
- [21] Bazylev V, Zhevago N 1987 *Emission From Fast Particles Moving in a Medium and External Fields* Moscow Nauka, 1987